Journal of Thermal Analysis, Vol. 32 (1987) 1039–1050

TRANSVERSE PHOTOTHERMAL DEFLECTION SPECTROSCOPY (PDS) APPLIED TO THERMAL DIFFUSIVITY MEASUREMENTS

G. Suber, M. Bertolotti, C. Sibilia, A. Ferrari***
and *F. Genel Ricciardiello****

SEZIONE FISICA, DIPARTIMENTO DI ENERGETICA, UNIV.
ROMA I, ROMA, ITALY
*FONDAZIONE U. BORDONI, ROMA
**DIPARTIMENTO DI FISICA, UNIV. NAPOLI
***ISTITUTO DI CHIMICA APPLICATA, UNIV. TRIESTE

(Received July 18, 1986)

Transverse photothermal deflection spectroscopy (PDS) is applied for the determination of thermal diffusivities of solid surfaces. The theory of PDS is briefly recalled and some approximated analytical formulae concerning the transverse configuration are derived. In materials where the thermal diffusivity is smaller than that of the air, the dependence of the deflection angle on the displacement between pump and probe beams is shown to have a minimum that relates to the thermal diffusivity, thereby allowing its straightforward measurement. Measurements carried out on Al_2O_3 samples with different porosities at room temperature show a good agreement between experiment and theory.

When an intensity-modulated beam of electromagnetic radiation (pump beam) impinges on an absorbing medium, heating will ensue. This time-dependent change of the medium temperature gives rise to a corresponding modulated index of refraction gradient which can be employed to deflect a probe beam travelling within the sample (collinear configwration Fig. 1a), or near the sample surface (transverse configuration Fig. 1b) [1]. This technique is usually indicated by the term photothermal deflection spectroscopy (PDS). The deflection angle so obtained depends on the thermal (diffusivity and conductivity) and optical parameters of the absorbing medium (absorption coefficient and reflectivity at the pump beam wavelength) [1], thereby allowing the PDS technique to be employed in the determination of such parameters [2, 3].

As long as thermal parameters are concerned, by measuring the amplitude and phase of the photothermal signal against the displacement between the pump and probe beams, the thermal diffusivity can be determined [2]. Further, in materials where the thermal diffusivity is smaller than that of the air, the transverse PDS

John Wiley & Sons, Limited, Chichester
Akadémiai Kiadó, Budapest

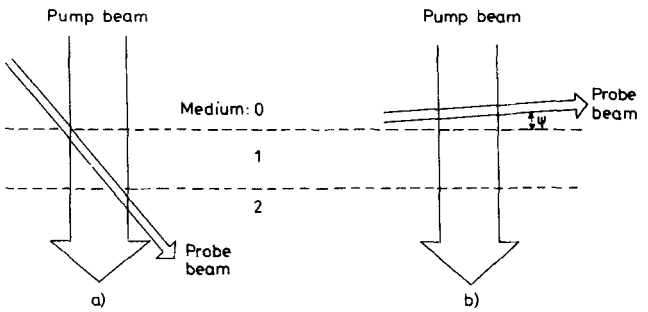

Fig. 1 Pump and probe beams relative positions in PDS (Photothermal Deflection Spectroscopy): a) collinear configuration; b) transverse configuration

signal plotted against the offset between the two beams shows a minimum that relates directly to the thermal diffusivity.

In the present paper we briefly recall the basic formulae of PDS and derive some approximated analytical expressions; we then show how the thermal diffusivity can be easily measured in an absolute way, and give some examples of diffusivity measurements on ceramic materials with various porosities.

Theory

The deflection angle is connected with the temperature gradient in the direction perpendicular to the probe beam path by the relation [1]:

$$\Phi = (1/n_0)(\partial n/\partial T) \int_{\text{path}} V_\perp T(\mathbf{r}, t)\, \mathrm{d}s \tag{1}$$

which in the case of the PDS transverse configuration with $\Psi = 0$ (Fig. 2) becomes:

$$\Phi = (1/n_0)(\partial n/\partial T) \int_{-\infty}^{+\infty} (\partial T_0(\mathbf{r}, t)/\partial z)\, \mathrm{d}x \tag{1'}$$

where n_0 and T_0 are the refractive index and temperature distribution of the medium crossed by the probe beam, i.e. the air in transverse configuration, when no heating occurs. Equation (1') can be integrated once the temperature distribution is determined by solving the heat equations:

$$\begin{aligned} \nabla^2 T_0 - (1/\chi_0)(\partial T_0/\partial t) &= 0 \\ \nabla^2 T_1 - (1/\chi_1)(\partial T_1/\partial t) &= -Q(\mathbf{r}, t)/k_1 \\ \nabla^2 T_2 - (1/\chi_2)(\partial T_2/\partial t) &= 0 \end{aligned} \tag{2}$$

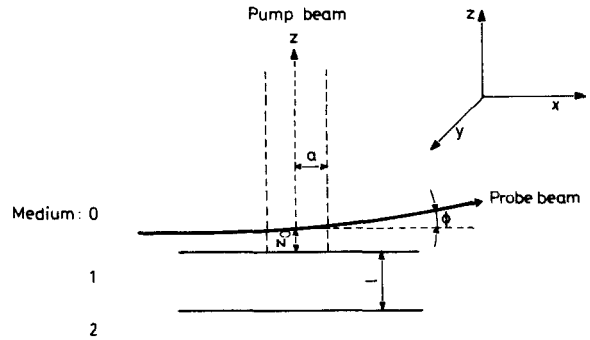

Fig. 2. PDS transverse configuration: the probe beam travelling in air at a mean distance z_0 from the sample surface is deflected by an angle Φ when the sample surface is heated by a Gaussian pump beam of radius a

with the boundary conditions:

$$T_0\Big|_{z=0} = T_1\Big|_{z=0}; \quad k_0(\partial T_0/\partial z)\Big|_{z=0} = k_1(\partial T_1/\partial z)\Big|_{z=0}$$
$$T_1\Big|_{z=1} = T_2\Big|_{z=1}; \quad k_1(\partial T_1/\partial z)\Big|_{z=1} = k_2(\partial T_2/\partial z)\Big|_{z=1} \tag{2'}$$

where T_i, χ_i and k_i are the temperature, thermal diffusivity and thermal conductivity of the i-th medium, respectively ($i=0, 1, 2$ see Fig. 2) and $Q(\mathbf{r}, t)$ is the heat deposited per unit volume. Equations (2) apply provided that only the sample is optically absorbing and all three media (air, sample and substrate) extend indefinitely in the radial direction.

If the pump beam is modulated by a chopper at the frequency ω, the heat deposited per unit volume in the sample, and thus the probe beam deflection angle, will oscillate at such frequency. For a sinusoidally-modulated Gaussian pump beam of radius a:

$$Q(\mathbf{r}, t) = 2P(1-R)\alpha/(\pi a)^2 \exp(-\alpha z) \exp(-2r^2/a^2) \exp(i\omega t) + c.c. \tag{3}$$

where P is the pump beam power on the sample of absorption coefficient α and reflectivity R.

Equations (2), with the boundary conditioos (2') and $QQ(\mathbf{r}, t)$ven by Eq. (3), lead to the temperature distribution in 0 medium (air [1]:

$$T_0(\mathbf{r}, t) = (1/2) \int_0^\infty \delta \, \mathrm{d}\delta \, J_0(\delta r) E(\delta) \exp(-\beta_0 z) \exp(i\omega t) + c.c. \tag{4}$$

with:

$$\beta_i^2 = \delta^2 + i\omega/\chi_i$$

$$E(\delta) = \Gamma(\delta) + A(\delta) + B(\delta)$$

$$\Gamma(\delta) = (P\alpha)\exp[-(\delta a)^2/8]/(\pi^2 k_1)(\beta_1^2 - \alpha^2)$$

$$A(\delta) = -[(1-g)(b-h)\exp(-\alpha 1) + (g+h)(1+b)\exp(\beta_1 1)]\Gamma(\delta)/H(\delta)$$

$$B(\delta) = -[(1+g)(b-h)\exp(\alpha 1) + (g+h)(1-b)\exp(-\beta_1 1)]\Gamma(\delta)/H(\delta)$$

$$H(\delta) = (1+g)(1+b)\exp(\beta_1 1) - (1-g)(1-b)\exp(-\beta_1 1)$$

$$g = k_0\beta_0/k_1\beta_1; \quad b = k_2\beta_2/k_1\beta_1; \quad h = \alpha/\beta_1$$

Therefore, the sample surface temperature $T_1(r, t) = T_0(r, t)$ becomes:

$$T_1(r, t) = (1/2)\int_0^\infty \delta\, d\delta\, J_0(\delta r)\, E(\delta)\exp(i\omega t) + c.c. \tag{5}$$

Equation (5) can be integrated in two approximations: 1. thin sample, 2. thick sample. Let l be the sample thickness and l_T its thermal diffusion length, $l_T = (2\chi_1/\omega)^{\frac{1}{2}}$. By a thin sample, we mean:

$$\alpha l \ll 1; \quad l \ll l_T$$

i.e. both optically and thermally thin, while for a thick sample the reverse applies, namely:

$$\alpha l \gg 1; \quad l \gg l_T$$

Further, for each approximation two different cases are taken into account:

i) $l_T \gg a$
ii) $l_T \ll a$

where a is the $1/e^2$ radius of the Gaussian pump beam. To achieve case i), a focussed pump beam and/or a high thermal conductivity of the sample and/or a low chopping frequency ω is needed, whereas case ii) requires the opposite conditions.

Table 1 gives temperature amplitudes of the sample surface calculated from Eq. (5) with the above-mentioned approximation. Table 2 gives deflection angle amplitudes calculated from Eqs (1′) and (4) with the same approximations as employed in Table 1. The linear behaviour with pump beam power P and the non-dependence on chopping frequency ω for $l_T \gg a$ should be noted.

Table 1 Temperature amplitude at the sample surface for a sinusoidal modulated pump beam

	$l_T \gg a$	$l_T \ll a$	
	(a)	(b)	
Thin slab	$\frac{\sqrt{2\pi}}{a}\frac{P(1-R)\alpha l}{\pi^2}\frac{e^{-\left(\frac{r}{a}\right)^2}}{k_0+k_2} I_0\left(\frac{r^2}{a^2}\right)$	$\frac{4P(1-R)\alpha l k_1}{\pi^2 a^2}\frac{e^{-2\left(\frac{r}{a}\right)^2}}{(A^2+(A+B)^2)^{1/2}}$	(*)
	(c)	(d)	
Thick slab	$\frac{\sqrt{2\pi}}{a}\frac{P(1-R)}{\pi^2}\frac{e^{-2\left(\frac{r}{a}\right)^2} I_0\left(\frac{r^2}{a^2}\right)}{k_0+k_1}$	$\frac{4P(1-R)\alpha}{\pi^2 a^2(k_0a_0+k_1a_1)}\frac{e^{-2\left(\frac{r}{a}\right)^2}}{(\alpha^2+(\alpha+2a_1)^2)^{1/2}}$	(**)

* $A = k_1(k_0a_0+k_2a_2)$; $B = 21(k_1^2a_1^2+k_0k_2a_0a_2)$.
** $a_i = (\omega/2\chi_i)^{1/2}$.

Table 2 Deflection angle amplitude for a sinusoidal modulated pump beam

	$l_T \gg a$	$l_T \ll a$	
	(a)	(b)	
Thin slab	$\frac{1}{n_0}\frac{\partial n}{\partial T}2\sqrt{\frac{2}{\pi^3}}\frac{P(1-R)\alpha l}{a(k_0+k_2)} e^{\frac{2z_0^2}{a^2}}\operatorname{erfc}\left(\frac{\sqrt{2}z_0}{a}\right)$	$\frac{1}{n_0}\frac{\partial n}{\partial T}2\sqrt{\frac{2}{\pi^3}}\frac{P(1-R)\alpha k_1 l a_0}{a}\frac{e^{-z_0a_0}}{((A+B)^2+B^2)^{1/2}}$	(*)
	(c)	(d)	
Thick slab	$\frac{1}{n_0}\frac{\partial n}{\partial T}2\sqrt{\frac{2}{\pi^3}}\frac{P(1-R)}{ak_1} e^{\frac{2z_0^2}{a^2}}\operatorname{erfc}\left(\frac{\sqrt{2}z_0}{a}\right)$	$\frac{1}{n_0}\frac{\partial n}{\partial T}2\sqrt{\frac{2}{\pi^3}}\frac{P(1-R)\alpha a_0}{a(a_0k_0+a_1k_1)}\frac{e^{-z_0a_0}}{((a_1+\alpha)^2+a_1^2)^{1/2}}$	(**)

* $A = k_1(k_0a_0+k_2a_2)$; $B = l(k_1^2a_1^2+k_0k_2a_0a_2)$.
** $a_i = (\omega/2\chi_i)^{1/2}$.

Experimental set-up

The experimental set-up for transverse PDS is outlined in Fig. 3.

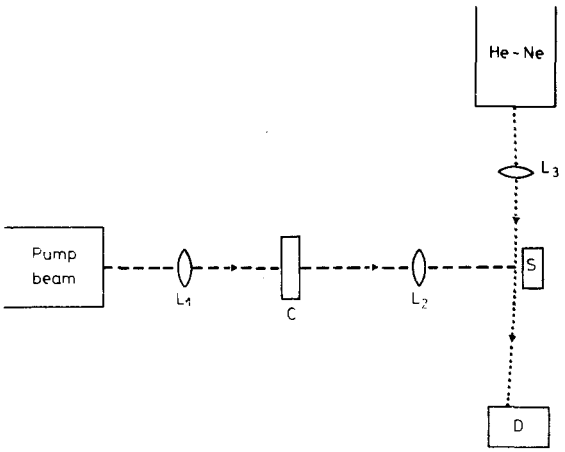

Fig. 3 Experimental set-up for transverse PDS: the pump beam modulated by a chopper C and focussed by lenses L_1 and L_2 impinges on the sample S where the He–Ne laser probe beam is focussed before reaching the detector D

The pump laser is a cw CO_2 laser and the detector a Si-photodiode with its sensitive surface half shut. By aligning the probe beam and the detector so that only half the intensity of the probe beam enters the detector when no heating occurs ($\Phi = 0$), a beam displacement is seen by the detector as an intensity change of the beam itself.

The probe beam intensity has the following radial behaviour:

$$I(r) = I(0) \exp(-2r^2/w_2^2)$$

for a Gaussian beam, where w_2 is the beam radius at the detector and $I(0)$ its intensity at the centre of the spot. When no heating occurs, the half-intensity of the probe beam is:

$$I_0 = \int_0^\infty I(r)\,dr = (1/2)(\pi/2)^{\frac{1}{2}} w_2 I(0)$$

The intensity variation ΔI corresponding to a displacement Δx of the beam at the detector is:

$$\Delta I/I_0 = (1/I_0) \int_0^{\Delta x} I(r)\,dr = \mathrm{erf}(\sqrt{2}\,\Delta x/w_2) \qquad (6)$$

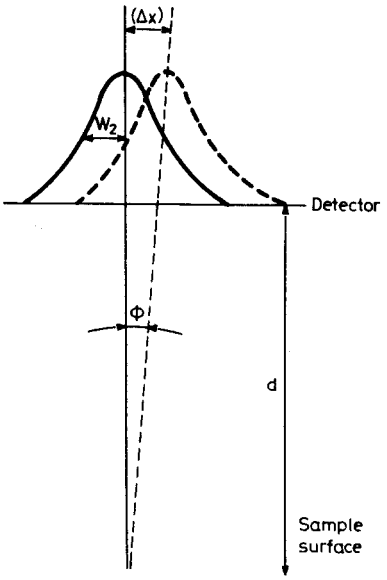

Fig. 4 Signal detection: a position displacement Δx of the probe beam intensity maximum at the detector is seen by the detector as an intensity change of the beam itself. Continuous curve: probe beam Gaussian profile at the detector when no heating occurs; dashed curve: the same profile when the beam is deflected by an angle Φ. w_2 is the probe beam radius at the focal spot and d the detector distance from the sample surface

For $z \ll 1$, $\mathrm{erf}(z) \simeq 2z/\sqrt{\pi}$ and consequently for $\Delta x \ll w_2$ Eq. (6) becomes:

$$\Delta I/I_0 = 2(2/\pi)^{\frac{1}{2}}(\Phi \pi w_0 n_0/\lambda)$$

with $\Delta x = \Phi d$ (Fig. 4), where d is the distance between the detector and the centre of the sample where the probe beam is focussed, and:

$$w_2 \simeq \lambda d/\pi w_0 n_0$$

with w_0 the radius at the focal spot and λ the probe beam wavelength. Therefore, the photodiode signal ΔV is connected with the deflection angle Φ by the relation [1]:

$$\Delta V/V = \Delta I/I = 2(2/\pi)^{\frac{1}{2}}(\pi w_0 n_0/\lambda)\Phi$$

which is independent on sample distance d.

To optimize the photothermal signal, the probe beam must travel as near as possible to the sample surface. This situation is outlined in Fig. 5, where the probe beam offset from the sample z_0 is given by:

$$z_0 = w_1 r_c/f \tag{7}$$

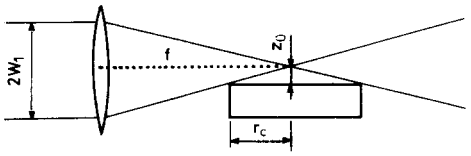

Fig. 5 The z_0 parameter. z_0 can be evaluated by simple geometrical considerations. w_1 is the radius of the Gaussian probe beam before being focussed by a f focal length lens on the sample of radius r_c

where w_1 is the probe beam radius in front of the f focus lens that focusses the beam on the sample, and r_c is the sample radius.

Finally, the detector output is connected both to a lock-in amplifier and to an oscilloscope to visualize the photothermal signal.

Thermal diffusivity measurements

Besides the thermal diffusivity χ_1, the deflection angles in Table 2 depend on other parameters of the sample, such as the reflectivity R, the absorption coefficient at the pump beam wavelength α and the thermal capacity ϱc or thermal conductivity k_1 as $\chi_1 = k_1(\varrho c)$.

For materials of unknown optical and thermal parameters, the thermal diffusivity can be determined as follows. If the displacement between the pump and probe beam intensity maxima is denoted by y_0, the simplest way to write the temperature distribution on the sample surface at a distance y_0 from the pump beam spot centre is as follows [2]:

$$T(r, t) = T_0 \exp(-y_0/l_T) \cos(\omega t - y_0/l_T) \tag{8}$$

where $T_0 = T(x, y_0 = 0, z, t = 0)$. In Eq. (8) y_0 is involved both in the amplitude of the temperature wave as an exponentially decreasing term, and in the phase as a delay term. Thus, the deflection angle will be (see Eq. (1')):

$$\Phi = (1/n_0)(\partial n/\partial T) \exp(-y_0/l_T) \cos(\omega t - y_0/l_T) \int_{-\infty}^{+\infty} (\partial T_0/\partial z)\, dx = \tag{9}$$

$$= \Phi_0 \exp(-y_0/l_T) \cos(\omega t - y_0/l_T)$$

with $\Phi_0 = \Phi(x, y_0 = 0, z, t = 0)$.

For $\chi_1 < \chi_0$, the absolute value of the in-phase signal of Eq. (9) with respect to y_0 has the general behaviour shown by the continuous curves in Figs 6a) and b). Note that for high χ_1; i.e. for $\chi_1 \gg \chi_0$, the second maximum due to the heat released by the previous energy pulse and still trapped in the sample disappears [1]. Further, the minimum between the two maxima directly relates to χ_1:

$$\chi_1 = (2\omega/\pi^2)(y_0^{\min})^2 \tag{10}$$

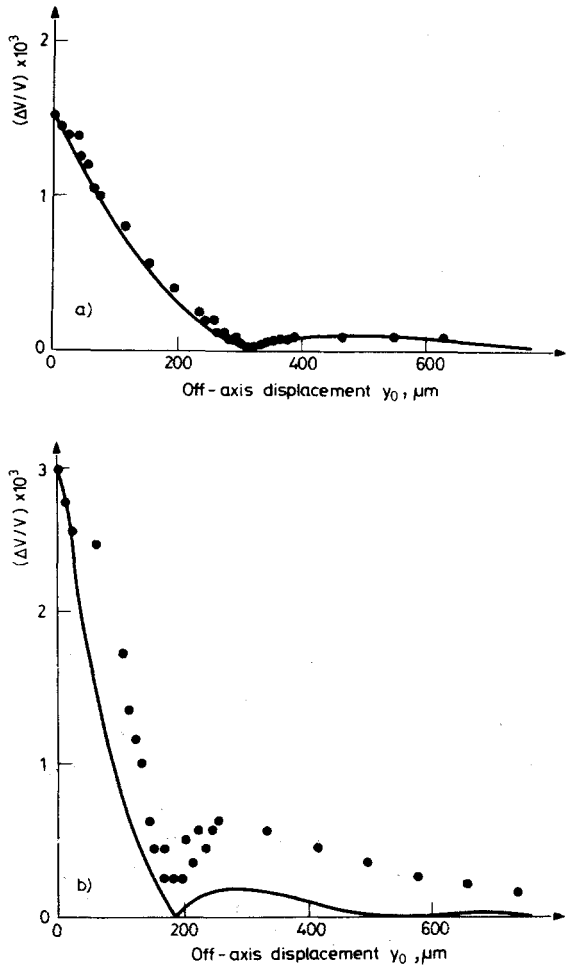

Fig. 6 Signal *vs.* off-axis displacement between pump and probe beams for Al_2O_3 samples of different porosity. Experimental points and theoretical behaviour: a) 51% porosity; b) 62% porosity

In order to test the method, sintered Al_2O_3 samples were employed. The CO_2 laser power on the sample was 50 mW, with a spot radius of 200 μm, while the probe beam focal spot radius was 20 μm. The temperature increase of the sample surface was estimated to be a few degrees. The displacement between the pump and probe beams was obtained by transversally moving the pump beam focussing lens, while leaving the probe beam travelling vertically near the sample surface unchanged. Figures 6a) and b) show the measured PDS signal against y_0 for Al_2O_3 samples of 51% and 62% porosity, respectively. The continuous curves in the same Figures

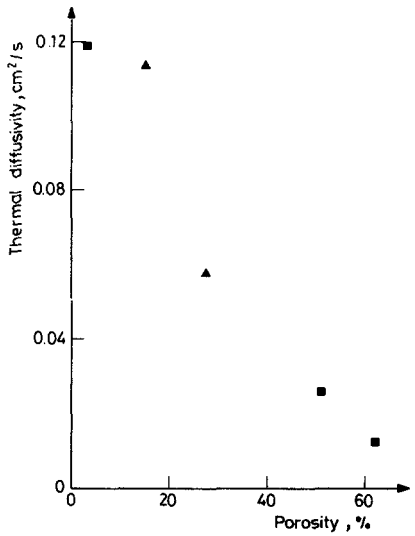

Fig. 7 Thermal diffusivity against porosity in Al_2O_3: (■) our measurements; (▲) R. Taylor measurements [4]

were obtained from the in-phase absolute value of Eq. (9) by fitting the central maximum and taking for the thermal diffusivity the values of 0.026 and 0.009 cm^2/s, respectively, which are derived from Eq. (10) with the experimental values of y_0^{min}. It should be noted that in Fig. 6a) the experimental points are in good agreement with the theoretical curve, while this is not true for Fig. 6b). A possible explanation of this behaviour is that in this case $l_T = (2\chi_1/\omega)^{1/2} = 120$ μm ($\omega = 20$ Hz) and for $l_T < a$ ($a = 200$ μm) the temperature-dependence on y_0 can no longer be factorized as in Eq. (8) and the Gaussian profile of the pump beam should be taken into account. In Fig. 8, the thermal diffusivity is given against porosity for three Al_2O_3 samples with porosities of 3%, 51% and 62%. The same Figure also reports two more values of thermal diffusivity measured by Taylor [4] for Al_2O_3 samples with porosities of 15% and 25–30%. Direct comparison of the values of thermal diffusivity we obtained and those reported in the literature is difficult, because of the differences in the preparation and in the porosity of the Al_2O_3 samples. This can be seen in Table 3, where Al_2O_3 thermal diffusivity measurements are given at room temperature, together with a few remarks about the sample preparation, porosity and particular method of measurement employed.

The error in the measured value of the thermal diffusivity can be estimated to be no more than 10%, which is due mostly to intensity fluctuations of the CO_2 pump laser, whereas the contribution to the error due to the indetermination of y_0 can be evaluated to be within 2%.

Table 3 Thermal diffusivity measurements of aluminium oxide (Al_2O_3) at room temperature

Thermal diffusivity, cm^2/s	Temperature, K	Remarks*
0.0830	298	a); pure; specimen a few mm's thick; extruded; plated with Hanovia Platinum Bright (No. 05); density 3.834 g cm^{-3}; high intensity, short duration, light pulse from Xe flash lamp absorbed in the front surface of thermally insulated specimen; thermal diffusivity determined from measured temperature history of the rear surface.
0.0687	293	a); pure; specimen a few mm's thick; pressed; plated with Hanovia Platinum Bright (No. 05); density 3.914 g cm^{-3}; heating source and thermal diffusivity determination as above.
0.093	298	a); specimen composed of three pieces; middle piece separated from bottom piece and upper piece by two 0.005 in. thick chromel sheets forming the heater; diffusivity determined from measured ratio of the temperature rises of the heat source and sink; density 3.04 g cm^{-3}; unidimensional heat flow.
0.114	298.2	a); 15% porosity-dense; measured mean density 3.23 g cm^{-3}; temperature of measurement not given by the author but assumed to be room temperature; heat pulse method used to measured diffusivity; cylindrical specimen 0.25 in. in diameter and 0.5 in. long.
0.058	298.2	a); 25–30% porosity; extruded or slip cast; measured mean density 2.86 g cm^{-3}; other conditions same as above.
0.091	298.2	a); 1.9 cm in diameter and 0.1 to 0.3 cm thick; density 3.51 g cm^{-3}.
0.0736	295	a); 8 mm in diameter and 2 to 5 mm thick.
0.119	298	b); 99% pure; sintered; 3% porosity; mean density 3.1 g cm^{-3}; 2 cm in diameter and 0.5 cm thick; diffusivity determined from PDS method.
0.026	298	b); 99% pure; sintered; 51% porosity; mean density 1.6 g cm^{-3}; 2.7 cm in diameter and 0.5 cm thick; diffusivity determined from PDS method.
0.009	298	b); 99% pure; sintered; 62% porosity; mean density 1.2 g cm^{-3}; 2.7 cm in diameter and 0.7 cm thick; diffusivity determined from PDS method.

* a) see Ref. [4], b) this work.

Conclusions

In this paper the PDS technique was applied for determination of the thermal diffusivity of solid surfaces. The thermal diffusivities of Al_2O_3 samples with different porosities were determined and seemed to match the values reported in the

literature, although a strict comparison is difficult because of the variations in the preparation and porosity of the Al_2O_3 samples.

Finally, it is interesting to compare PDS briefly with the method most often employed for thermal diffusivity measurements, i.e. the "flash" method (rear face monitoring) [5, 6]. This latter method has been employed for over 20 years, during which it has undergone many improvements concerning the formulation of a more "realistic" theory where actual measurement conditions are taken into account. For example, the theory of the "flash" method applied for a Dirac pulse and for samples absorbing optical radiation at their surface, so that effects due to the finite duration of the laser pulse and to the optical transmission of laser radiation through the sample must be considered. As ceramic materials often show optical transmission, in the "flash" method they are usually coated with a film of a well-conductive material, such as platinum, that involves a possible imperfect contact at the interface. In contrast, neither the finite duration of the laser pulse nor optical transmission through the sample obviously affect PDS. The lack of such effects prove the use of the PDS method for thermal diffusivity measurements, especially in relation to ceramic materials.

References

1 W. B. Jackson, N. M. Amer, A. C. Boccara and D. Fournier, Appl. Opt., 20 (1981) 1333.
2 N. M. Amer, Ing. Nucl., 3 (1985).
3 A. C. Boccara, D. Fournier, W. B. Jackson and N. M. Amer, Opt. Lett., 5 (1980) 377.
4 Y. S. Touloukian, Thermophysical Properties of High Temperature Materials, McMillan, New York 1974.
5 A. Degiovanni, Rev. Gen. Thermique, 185 (1977) 420.
6 D. L. Balageas, Tire a Part ONERA No. 1984–144, Chatillon, France 1984.

Zusammenfassung — Die transverse photothermische Reflektionsspektroskopie (PDS) wird zur Bestimmung der thermischen Diffusivität von festen Oberflächen herangezogen. Die Theorie der PDS wird kurz dargelegt und einige sich auf die transverse Konfiguration beziehenden analytischen Näherungsgleichungen abgeleitet. Es wird gezeigt, daß bei Materialien mit kleinerer thermischer Diffusivität als Luft die Abhängigkeit des Deflektionswinkels von der Ablenkung zwischen Pumpen- und Probenstrahl ein Minimum aufweist, das mit der thermischen Diffusivität im Zusammenhang steht und somit deren zuverlässige Messung ermöglicht. An Al_2O_3-Proben unterschiedlicher Porosität bei Raumtemperatur ausgeführte Messungen zeigen gute Übereinstimmung von Experiment und Theorie.

Резюме — Фототермическая спектроскопия поперечного отклонения была использована для определения термических коэффициентов диффузии твердых поверхностей. В краткой форме приведена теория фототермической спектроскопии поперечного отклонения и выведены некоторые приближенные аналитические формулы, касающиеся поперечной конфигурации. В случае веществ, для которых термический коэффициент диффузии меньше, чем для воздуха, зависимость угла отклонения от смещения между лучом накачки и пробы показывает минимум, что связано с термическим коэффициентом диффузии и таким образом представляется возможность его прямого измерения. Измерения, проведенные при комнатной температуре с образцами окиси алюминия различной пористости, показали хорошее совпадение между теорией и экспериментом.